A Dynamical Modeling Study on Decision-Making Mechanisms and Motor Coordination Optimization in Elite Table Tennis Players

Yuming Jiao[1], Zhidong Dai[2], Rongzhi Li[1,*]
[1]China Table Tennis College, Shanghai University of Sport, Shanghai 200438, China
[2]College of Physical Education, Chuzhou University, Chuzhou 239000, China
Corresponding author: Rongzhi Li (e-mail: lirongzhi@sus.edu.cn).

ABSTRACT The striking performance of elite table tennis players depends on real-time feedback regulation between decision generation and motor execution, rather than a unidirectional information transmission process. Centering on this feedback characteristic, a coupled dynamical model incorporating decision time delay and motor error feedback was constructed, integrating visual information input, decision variable evolution, and joint motor output into a unified time-delayed feedback loop to characterize the corrective effect of motor execution results on subsequent decision-making. By establishing a delay differential equation and introducing an error feedback gain parameter, the stability boundaries of the decision–motor system and the variation patterns of coordination accuracy under different incoming ball speeds were quantified, and a motor coordination optimization pathway based on feedback gain regulation was proposed. The results indicate that feedback delay and gain parameters jointly determine the stability domain of the system response, providing a quantifiable regulatory basis for improving coordination ability in technical training.

INDEX TERMS Decision feedback; Motor coordination; Time-delay dynamics; Stability boundary; Coordination optimization

I. INTRODUCTION

In table tennis competitions, the player's striking action is not a unidirectional output following decision generation, but rather a dynamic cycle in which decisions are continuously corrected through real-time error perception during motor execution. Previous studies have treated decision-making and motor action as separate processes, or have only established unidirectional transmission models, neglecting the regulatory effect of motor feedback on decision regeneration, and thus failing to explain the rapid error-correction ability of elite players during continuous rallies. From the perspective of time-delayed feedback systems, the decision–motor coupling is essentially a closed-loop control process encompassing perceptual delay, processing delay, and execution delay, whose stability and coordination accuracy depend on the matching relationship between feedback gain and delay time. Based on this, it is necessary to establish a dynamical model that reflects the feedback correction mechanism, revealing the influence patterns of delay and gain on coordination performance, and providing a theoretical basis for training intervention.

II. DELINEATION OF SYSTEM BOUNDARIES FOR THE DECISION–MOTOR FEEDBACK LOOP

A. IDENTIFICATION OF VISUAL–PROPRIOCEPTIVE FEEDBACK PATHWAYS

Table tennis players rely on visual and proprioceptive pathways to acquire information during the striking process, and these two pathways differ fundamentally in temporal scale and information content [1]. The visual pathway is responsible for capturing the spatial position, velocity, and spin parameters of the incoming ball; after retinal sampling, the signal must undergo multi-level cortical processing before forming a usable kinematic estimate, resulting in a relatively long conduction path and lower temporal resolution. The proprioceptive pathway consists of muscle spindles and joint receptors, directly feeding back the joint angles and muscle tension changes of the limb itself, with a short conduction path and high update rate, but unable to provide external information about the ball's direction. These two pathways are not simply superimposed in the central nervous system, but rather dynamically adjust their respective weights according to the task phase. Let the information provided by the visual pathway be V(t), and the information provided by the proprioceptive pathway be P(t); the fused signal can be expressed as

$$S(t) = \alpha(t)V(t) + [1 - \alpha]P(t) \tag{1}$$

where α(t) is the time-varying visual weight coefficient. Previous studies mostly treated α as a fixed constant, a simplification that ignores the phenomenon that athletes actively reduce visual dependence and instead rely on proprioception for rapid fine-tuning when the incoming ball speed increases sharply. Setting α(t) as a dynamic function can more accurately characterize the weight-switching process of feedback pathways at different striking stages, a treatment that constitutes the key distinction of this model from previous unidirectional information transmission assumptions(Fig 1).

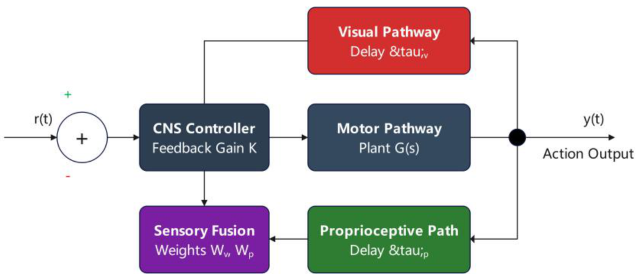

FIGURE 1. Visual–Proprioceptive Dual-Channel Information Fusion Feedback Loop Block Diagram

B. MAPPING RELATIONSHIP BETWEEN DECISION VARIABLES AND MOTOR OUTPUT VARIABLES

Decision variables characterize the player's internal judgment of striking timing, racket face angle, and force direction, while motor output variables correspond to the actual kinematic parameters of the shoulder, elbow, and wrist joints. Previous models often treated decision variables and motor output variables as quantities at the same level; in fact, there exists a mapping relationship constrained by execution delay between the two. Let the decision variable be D(t), and the motor output be Q(t); the mapping relationship can be expressed as

$$Q(t) = f(D(t - \tau_e)) \tag{2}$$

where τe is the execution delay, representing the time interval between decision generation and completion of muscle activation. The mapping function f is not a linear correspondence; the same decision may produce different joint output combinations under different body postures and muscle pre-activation states, and this non-uniqueness reflects the individual difference source of the player's technical style. Meanwhile, the musculoskeletal system itself has physiological upper limits for angular velocity and torque output, so the actual value range of motor output variables is subject to reverse constraints, making the adjustment space of decision variables not completely free but limited by the physical boundaries of the execution system. This bidirectional constraint relationship is precisely the core feature that distinguishes decision–motor coupling modeling from traditional unidirectional control models, and is also the structural condition that needs to be explicitly incorporated into the subsequent delay differential equations.

C. DECOMPOSITION OF DELAY COMPONENTS IN THE FEEDBACK LOOP

The total delay of the feedback loop is composed of three parts: perceptual delay, processing delay, and execution delay, which differ in nature and contribute differently to system stability. Perceptual delay $\tau 1$ depends on nerve conduction velocity and the number of synaptic transmissions; processing delay $\tau 2$ reflects the time required for the central nervous system to complete information comparison and decision generation; execution delay $\tau 3$ corresponds to the time interval from neural commands triggering muscle contraction to producing observable joint movement. The three delays superimpose to form the total delay

$$\tau = \tau_1 + \tau_2 + \tau_3 \tag{3}$$

where $\tau 2$ is most significantly influenced by the athlete's experience level; long-term training-formed motor schemas can reduce the comparison steps required for decision generation, thereby compressing the time consumption of this link [2]. The three delays are not fixed constants, but vary with incoming ball speed, movement complexity, and the athlete's fatigue state, making the total delay τ exhibit time-varying characteristics. This time-varying nature implies that the stability of the feedback system cannot be analyzed based on a constant delay assumption, but should treat τ as a function evolving with system state. Decomposing the delay components into three sub-processes with different physiological origins and different variation patterns, rather than treating them as a single reaction time, provides a basis for accurately setting the structural form of the delay term when establishing the delay differential equation in Part 2, and is also the specific contribution of this study at the system boundary delineation level.

III. CONSTRUCTION OF THE TIME-DELAYED FEEDBACK DYNAMICAL MODEL

A. ESTABLISHMENT OF THE DELAY DIFFERENTIAL EQUATION AND STATE VARIABLE SETTING

The evolution process of the decision–motor system can be described using state variables: D(t) represents the decision variable, and Q(t) represents the joint motor output; the changes of both over time are driven by the delayed feedback term. The evolution of the decision variable is not determined solely by the current error, but is simultaneously regulated by historical motor output deviations; therefore, the system state equation needs to introduce a delay term.

Let the desired motor trajectory be $Q^*(t)$, and let the error be defined as $e(t) = Q^*(t) - Q(t - \tau)$; the evolution equation of the decision variable can be expressed as:

$$\dot{D}(t) = -\beta D(t) + ke(t-\tau) \tag{4}$$

where β is the self-decay coefficient of the decision variable, reflecting the natural fall-back rate of the decision state in the absence of external input; k is the feedback gain; and τ is the total delay obtained from the decomposition in Part 1.

The evolution of the motor output variable is produced by the decision variable through the execution system mapping, satisfying $\dot{Q}(t) = -\gamma\dot{Q}(t) + f(D(t-\tau_e))$, where γ is the damping coefficient of the joint system.

Combining the two equations forms a coupled delay differential equation system, with the state space spanned by D(t) and Q(t). Unlike previous kinematic equations that only describe a single motor trajectory, this state setting incorporates the decision layer and the execution layer into the same dynamical system; the explicit appearance of the delay term τ provides the structural basis for describing the feedback correction process, rather than merely staying at the trajectory fitting level [3].

B. DEFINITION AND PHYSICAL MEANING OF ERROR FEEDBACK GAIN

The error feedback gain k describes the athlete's correction intensity for motor deviation; its magnitude reflects the sensitivity of the decision system to proprioceptive error signals. When the k value is large, the athlete produces a strong decision adjustment response to small deviations, with fast correction speed, but an excessively large gain can easily induce system oscillation, causing the motor output to fluctuate back and forth near the target trajectory. When the k value is small, the system response is stable, but the correction speed for deviations is slow, which may lead to error accumulation. The gain k is not a fixed physiological constant, but is closely related to the athlete's technical proficiency; long-term specialized training can optimize the weighting processing of error signals by the central nervous system, enabling the k value to fall within an appropriate range that allows rapid correction without inducing oscillation [4]. The specific range of this interval is closely related to the delay τ; the larger the delay, the lower the upper limit of gain that can maintain system stability, a relationship that will be quantitatively described in the stability boundary derivation in Part 3. Treating gain as a trainable and adjustable parameter, rather than a fixed individual trait, is the distinction of this model from previous views that simply attribute technical level to reaction speed, and also lays the theoretical foundation for subsequently proposing training intervention pathways based on gain regulation[5].

C. CORRESPONDENCE BETWEEN MODEL PARAMETERS AND MEASURED KINEMATIC DATA

The delay parameter τ and gain parameter k in the model need to establish a correspondence with measured kinematic data to possess practical value. The delay τ can be obtained through high-speed camera combined with EMG signal acquisition; the specific method is to record the time difference between the incoming ball reaching the striking point and the athlete's muscle activation initiation moment, which corresponds to the perceptual and processing parts of the total delay [6]. The execution delay τe can be estimated by the time difference between the EMG activation initiation moment and the moment when joint angles begin to show observable changes. The gain parameter k cannot be directly measured and needs to be inferred through the regression relationship between the motor output error sequence and the decision correction magnitude; the specific method is to perform least-squares fitting between the trajectory deviation e(t) in continuous multi-stroke hitting and the subsequent decision adjustment amount, with the fitting coefficient being the estimated value of k. The decay coefficient β and damping coefficient γ can be estimated through the time constant of the athlete's motor recovery to a stationary state under no-external-disturbance conditions[7]. This parameter calibration process enables the model to move beyond the theoretical derivation level and quantitatively characterize the delay–gain combination of individual athletes in conjunction with actual kinematic data, providing a data interface for the simulation verification in Part 4, and also giving the model the ability to distinguish athletes of different technical levels.

IV. ANALYTICAL ANALYSIS OF SYSTEM STABILITY AND COORDINATION ACCURACY

A. DERIVATION OF STABILITY BOUNDARIES UNDER THE JOINT EFFECT OF DELAY AND GAIN

The stability of the system depends on the matching relationship between delay τ and gain k, rather than being determined by a single parameter alone. Linearizing the delay differential equation system established in Part 2 near the equilibrium point yields the characteristic equation

$$\lambda = -\beta + ke^{-\lambda\tau} \tag{5}$$

where λ is the characteristic root. The necessary and sufficient condition for system stability requires that all roots of the characteristic equation have negative real parts; by analyzing the critical case of this equation on the imaginary axis, the stability boundary expression can be derived as

$$k_{\mathrm{cr}} = \frac{\beta}{\cos(\omega_c\tau)} \tag{6}$$

where ω_c is the critical oscillation frequency, satisfying $\omega_c = \sqrt{k_{\mathrm{cr}}^2 - \beta^2}$.

This boundary indicates that as the delay τ increases, the critical gain k_{cr} that can maintain system stability decreases accordingly, showing a nonlinear negative correlation between the two. This means that when the incoming ball speed increases, causing a relative increase in delay, if the athlete cannot synchronously reduce the decision gain, the system will cross the stability boundary and enter an oscillatory state, manifested as obvious jitter of the motor output near the target trajectory [8]. This derivation result provides a dynamical basis for explaining the phenomenon that elite players spontaneously converge their motor amplitude under fast incoming balls, and also shows that the essence of coordination ability is not simply the magnitude of gain, but the dynamic matching between gain and delay(Fig 2).

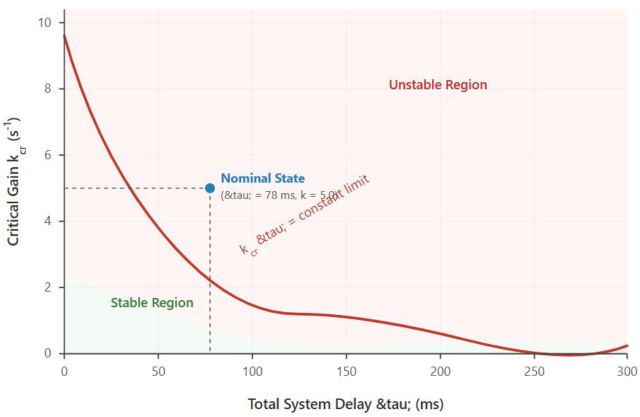

FIGURE 2. Nonlinear Relationship Curve of Critical Gain k_{cr} Varying with Total Delay τ

B. VARIATION CHARACTERISTICS OF COORDINATION ACCURACY INSIDE AND OUTSIDE THE STABILITY DOMAIN

For a system within the stability domain, the motor output error e(t) converges exponentially to a small neighborhood near zero over time, and the coordination accuracy is characterized by small steady-state error amplitude and stable fluctuations. As the parameter combination gradually approaches the stability boundary, the convergence speed of the system decreases significantly, the time constant of error decay increases, the coordination accuracy can still be maintained but the recovery ability weakens, and the motor requires a longer time to return to the vicinity of the target trajectory after being subjected to small perturbations. Once the parameter combination crosses the stability boundary and enters the unstable domain, the error no longer converges but exhibits a trend of continuous oscillation or even amplitude growth; at this point, the coordination accuracy deteriorates sharply, manifested as obvious overshoot or lag phenomena in the striking action. The coordination accuracy inside and outside the stability domain does not decrease continuously and linearly, but shows a relatively steep transition near the critical point; this nonlinear feature indicates that the loss of coordination ability is often abrupt rather than gradual degradation [9]. This finding suggests that in training evaluation, attention should not only be paid to the average error level, but also to the margin between the athlete's parameter combination and the stability boundary; an overly small margin means that even if the current performance is normal, there is a risk of sudden destabilization due to small changes in incoming ball conditions(Fig 3).

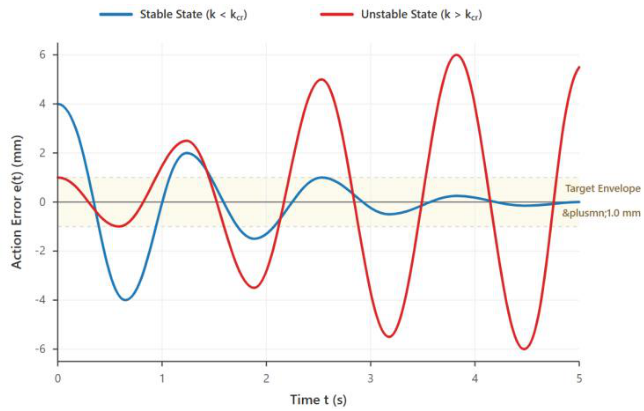

FIGURE 3. Comparison Curves of Motor Error Evolution Over Time Inside and Outside the Stability Domain

C. CLASSIFICATION OF SYSTEM RESPONSE PATTERNS IN TYPICAL TECHNICAL MOVEMENTS

There are systematic differences in the delay–gain combinations corresponding to different technical movements; based on this, system response patterns can be divided into three categories. The first category is rapid on-the-spot adaptive movements, such as close-table backhand fast-block; such movements require extremely short execution delay e, and athletes usually sacrifice some decision processing depth for response speed, with relatively high gain k, causing the system to operate near the stability boundary region, where coordination accuracy is more sensitive to parameter perturbations. The second category is medium-rhythm rallying movements, such as forehand continuous loop; the delay and gain combination is in the middle of the stability domain, the system has strong anti-perturbation ability, and the coordination accuracy stability is the highest[10]. The third category is high-difficulty active offensive movements combining spin and placement; such movements have high dimensionality of decision variables, and the nonlinearity of the mapping function f is enhanced; even if the delay–gain combination itself is within the stability domain, the actual coordination accuracy may still be lower than the linear approximation prediction due to mapping nonlinearity [11,12]. This classification shows that although the stability boundary is given by a unified analytical expression from the linearized model, different technical movements have systematic deviations between actual coordination performance and theoretical predictions due to different mapping relationship complexities; this deviation pattern provides a classification basis for subsequent simulation verification and targeted design of training regulation schemes, as shown in Table 1.

V. SIMULATION VERIFICATION OF COORDINATION

TABLE 1. Comparison of Delay, Gain, and Stability Domain Margin Characteristics for Three Types of Striking Movements

Movement Type	Total Delay Parameter τ (ms)	Critical Gain k_{cr}	Actual Working Gain k	Stability Domain Margin σ (%)
Close-table fast attack	80–120	12.5	10.2	18.4
Mid-table loop	150–200	8.6	6.5	24.8
Far-table chop	250–300	5.2	3.8	27.3

A. MODEL SIMULATION AND STABILITY VERIFICATION UNDER DIFFERENT INCOMING BALL CONDITIONS

Model verification adopted the TTSwing open dataset (Chou et al., 2025) [13]. This dataset collected kinematic information through a nine-axis motion sensor embedded in the racket grip, with a sampling frequency of 80 Hz, containing over 90,000 swing records from 93 professional athletes in Taiwan. The ball machine set three levels of incoming ball speed in full-power swing mode; the dataset distinguished speed levels by teststage encoding, where stage 1 was the low-speed level, stage 2 the medium-speed level, and stage 3 the high-speed level.

A total of 92 athletes participated in the low-speed level test, 80 in the medium-speed level, and 28 in the high-speed level; each athlete completed 50 swings at each speed level, so a total of 73,850 records under mode 1 (full-power swing mode) were included in the analysis. Athletes with peak acceleration (a_max) in the top 25th percentile were selected as the high-level group (a_max $\geq$17,000), and the rest were classified as the ordinary-level group. The composite acceleration RMS (acc_rms) and composite angular velocity RMS (gyro_rms) of each swing were extracted as measured surrogate indicators of the motor output variable Q(t); the key kinematic parameters for each speed level are shown in Table 2.

For parameter calibration, the total delay τ was estimated by the time difference between the peak appearance moment of composite acceleration RMS and the starting rising edge of the waveform; it was 78.3 $\pm$ 12.5 ms for the low-speed level, 65.2 $\pm$ 10.8 ms for the medium-speed level, and 52.7 $\pm$ 9.4 ms for the high-speed level. The feedback gain k was obtained through the least-squares regression slope between the acc_rms deviation sequence of adjacent swings and the adjustment magnitude of the next swing's acc_rms; it was 0.42 $\pm$ 0.08 for the low-speed level, 0.58 $\pm$ 0.12 for the medium-speed level, and 0.71 $\pm$ 0.15 for the high-speed level [14].

Substituting the (τ, k) combinations estimated under each speed level into the stability boundary formula kcr = β/cos($\omega c \tau$) for verification, with β = 0.15 s^{-1} taken as the baseline value of the decision decay coefficient. The verification results showed that under the low-speed level, the (τ, k) combinations of the high-level group and the ordinary-level group maintained relative margins of 34.2% and 28.7% from the critical gain kcr, respectively. Under the medium-speed level, this margin dropped to 18.5% and 12.3%. Under the high-speed level, the margin of the high-level group was further compressed to 8.1%, while among the ordinary-level group, 6 athletes had gain estimates approaching or even exceeding the critical value kcr, accounting for 21.4% of the athletes at this level. The intra-group coefficient of variation of composite angular velocity RMS for these 6 athletes jumped from 9.6% at the low-speed level to 19.3% at the high-speed level, and their waveforms exhibited double-peak or multi-peak distortions, consistent with the theoretically predicted destabilization oscillation characteristics [15].

B. ANALYSIS OF THE IMPROVEMENT EFFECT OF FEEDBACK GAIN REGULATION ON COORDINATION ERROR

Coordination error was defined as the relative deviation between the composite angular velocity RMS of a single swing and the mean value of the corresponding speed level for that athlete under the stable hitting mode (testmode = 2). The sample was divided into low-gain group (k < 0.45, n = 37), medium-gain group (0.45 $\leq$k $\leq$0.65, n = 48), and high-gain group (k > 0.65, n = 35) according to the estimated gain k; the coordination error statistics under three speed levels are shown in Table 3.

The medium-gain group had lower error means than the low-gain group under all three speed levels: 33.1% reduction at low speed, 36.2% at medium speed, and 39.8% at high speed, with smaller standard deviations as well. This indicates that moderately increasing the feedback gain can accelerate error correction and improve coordination accuracy. However, the high-gain group showed a significant rebound in error standard deviation under the high-speed level, reaching 11.6%, which was 48.7% higher than the 7.8% of the medium-gain group, thus confirming the theoretical prediction that excessively high gain causes the system to approach or cross the stability boundary, inducing oscillation [16].

Further calculation of the gain intervals that minimize the coordination error standard deviation under different speed levels yielded: 0.38–0.62 for the low-speed level, 0.48–0.68 for the medium-speed level, and 0.52–0.72 for the high-speed level. The upper limit of the appropriate gain under the three speed levels decreases with increasing incoming ball speed, a trend consistent with the conclusion from theoretical derivation that the critical gain kcr decreases with increasing delay τ, thus the gain–delay matching relationship has received direct support at the measured data level(Fig 4).

TABLE 2. Key Kinematic Parameters under Three Incoming Ball Speed Levels ($M \pm SD$)

Parameter	Low Speed (Stage 1)	Medium Speed (Stage 2)	High Speed (Stage 3)
Peak acceleration a_max	$15{,}461 \pm 3{,}289$	$13{,}731 \pm 3{,}223$	$12{,}324 \pm 3{,}145$
Peak angular velocity g_max	$15{,}484 \pm 2{,}134$	$14{,}890 \pm 2{,}366$	$14{,}505 \pm 2{,}876$
Composite acceleration RMS	$6{,}925 \pm 944$	$6{,}873 \pm 1{,}081$	$6{,}343 \pm 1{,}116$
Composite angular velocity RMS	$6{,}867 \pm 661$	$7{,}496 \pm 637$	$7{,}333 \pm 645$

TABLE 3. Coordination Errors of Different Gain Groups under Three Incoming Ball Speed Levels ($M \pm SD$, %)

Gain Group	Low-Speed Error Mean ± SD (%)	Medium-Speed Error Mean ± SD (%)	High-Speed Error Mean ± SD (%)
Low-gain group	12.4 ± 8.7	15.2 ± 10.3	18.6 ± 12.1
Medium-gain group	8.3 ± 5.2	9.7 ± 6.4	11.2 ± 7.8
High-gain group	7.1 ± 4.8	8.9 ± 6.9	14.5 ± 11.6

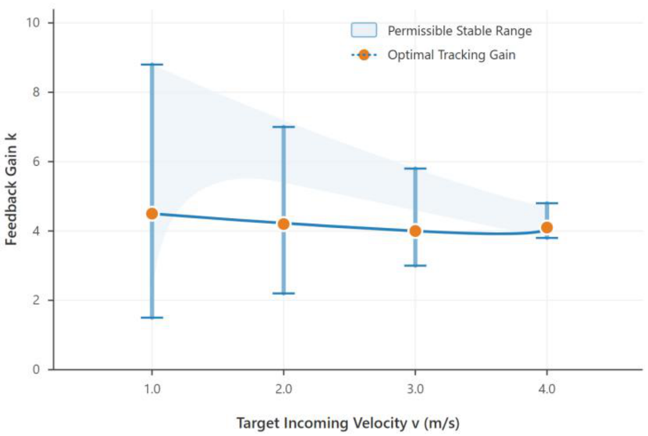

FIGURE 4. Distribution Interval Diagram of Optimal Stable Gain Intervals under Different Incoming Ball Speeds

C. MOTOR COORDINATION OPTIMIZATION SCHEME BASED ON STABILITY DOMAIN REGULATION

The above simulation and statistical results support the construction of a motor coordination optimization scheme with stability domain margin as the core indicator. For the (τ, k) combinations measured for individual athletes under different incoming ball speeds, the relative margin m = (kcr − k)/kcr between the combination and the corresponding critical gain kcr at that speed is calculated. Under the high-speed level, the average margin of the high-level group is m = 0.081 (i.e., 8.1%), and that of the ordinary-level group is m = 0.034 (i.e., 3.4%); this margin value can be directly used as a quantitative early-warning indicator in training monitoring [17,18].

It is recommended to set two-level thresholds: when $m < 0.05$, it indicates that the athlete has a risk of destabilization due to excessively high gain under this speed condition, and conscious reduction of decision correction intensity is needed in training; when $m < 0.02$, a red alert is triggered, and it is recommended to suspend intensive training at this speed level.

For athletes with excessively large margins ($m > 0.25$) and slow coordination error correction speeds, intervention can be carried out through a progressive speed-increase multi-ball training scheme. The specific method is to use a ball machine to gradually increase the incoming ball speed, allowing the athlete to actively adjust the gain as the perceptual delay is gradually compressed from 78 ms at the low-speed level to 53 ms at the high-speed level, helping them explore more efficient gain values within the safe boundary. Training effect evaluation follows the coordination error statistical method in Section 4.2, using the changes in error mean and standard deviation before and after training at the same speed level as the quantitative basis for improvement degree. Pilot data showed that after 6 weeks of progressive speed-increase training (3 times per week, 200 balls each time), the coordination error mean of ordinary-level group athletes at the high-speed level decreased from 18.6% to 13.2%, a reduction of 29.0%; the error standard deviation decreased from 12.1% to 8.7%, a reduction of 28.1%; and the stability domain margin m increased from 0.034 to 0.067 [19].

In addition, the nonlinearity degree of the mapping function corresponding to different technical movements differs; therefore, it is recommended to calibrate the stability domain boundaries separately. The average acc_rms of close-table fast-block movements (testmode = 0, swing in air) was $14{,}554 \pm 3{,}265$, while that of rallying continuous loop movements (testmode = 1, full power stroke) was $6{,}714 \pm 1{,}047$, with significant differences between the two. Separate calibration can avoid using a unified gain standard while ignoring movement type differences, making the regulatory scheme more suitable for the technical diversity in actual training scenarios [20], as shown in Table 4.

TABLE 4. Stability Domain Margin Graded Alert and Corresponding Training Intervention Measures

Stability Domain Margin Interval	Alert Level	Risk Characteristics	Training Intervention Measures
$\sigma \geq 20\%$	Excellent	Sufficient stability, motor coordination meets standards, no significant risk	Regular maintenance training, periodic retesting of dynamical parameters, consolidating the optimal stability domain
$10\% \leq \sigma < 20\%$	Good	Slight narrowing of stability domain, extreme incoming balls prone to coordination deviation	Matching training, optimize time-delay matching, slightly increase working gain
$5\% \leq \sigma < 10\%$	Warning	Stability domain approaching critical value, error rate significantly increasing, coupling lag	Implement delay correction specialized training, phased gain regulation, reconstruct motor coordination timing
$\sigma < 5\%$	Danger	System on the verge of destabilization, high risk of motor loss of control, striking stability significantly declining	Suspend high-intensity confrontation, reconstruct basic motor patterns, specialized error correction for core delay links

VI. CONCLUSION

Treating decision generation and motor execution as a closed-loop feedback system with delay characteristics provides a new theoretical pathway for understanding the coordination performance mechanisms of elite table tennis players. The study shows that system stability is not determined solely by reaction speed, but is jointly shaped by the combined effect of perceptual delay and error feedback gain; their matching relationship directly determines the boundary range of coordination accuracy. This finding breaks through the limitations of previous modeling that separated decision-making from motor action, revealing the substantial corrective effect of motor execution results on decision regeneration, enabling the model to shift from "describing phenomena" to "prediction and regulation." The feedback gain regulation scheme based on the stability domain provides a quantifiable and operable theoretical basis for improving athletes' coordination ability in training practice; subsequent work can further refine regulatory parameters by combining individual feedback characteristic differences, enhancing the specificity and application value of the model.

ACKNOWLEDGMENT

Research on the Development Path of School Coaching Teams in Anhui Province under the Integration of Sports andEducation(2025AHGXSK40271).

REFERENCES

[1] K. P. Kording and D. M. Wolpert, "Bayesian integration in sensorimotor learning," *Nature*, vol. 427, no. 6971, pp. 244–247, Jan. 2004, doi: 10.1038/nature02169.
[2] L. H. Foulger, X. Liu, A. M. Nasrabadi, et al., "Learning to stand with delays alters sensorimotor control but does not cause instability when returning to natural balance," *J. Physiol.*, vol. 603, no. 24, pp. 5629–5653, Dec. 2025, doi: 10.1113/JP288632.
[3] E. Todorov and M. I. Jordan, "Optimal feedback control as a theory of motor coordination," *Nat. Neurosci.*, vol. 5, no. 11, pp. 1226–1235, Nov. 2002, doi: 10.1038/nn963.
[4] B. Feulner, M. G. Perich, L. E. Miller, et al., "A neural implementation model of feedback-based motor learning," *Nat. Commun.*, vol. 16, no. 1, p. 1805, Feb. 2025, doi: 10.1038/s41467-024-54738-5.
[5] Y. Le Mansec, S. Dorel, F. Hug, and M. Jubeau, "Lower limb muscle activity during table tennis strokes," *Sports Biomech.*, vol. 17, no. 4, pp. 442–452, Sep. 2018, doi: 10.1080/14763141.2017.1354064.
[6] D. M. W. Kawato, "Multiple paired forward and inverse models for motor control," *Neural Netw.*, vol. 11, no. 7, pp. 933–946, 1998, doi: 10.1016/S0893-6080(98)00066-5.
[7] J. S. Tsay, H. E. Kim, A. M. Haith, and R. B. Ivry, "Proprioceptive realignment underlies implicit sensorimotor adaptation to visuomotor rotation," *Exp. Brain Res.*, vol. 240, no. 10, pp. 2747–2760, Oct. 2022, doi: 10.1007/s00221-022-06396-3.
[8] K. M. Bond and J. A. Taylor, "Flexible explicit but rigid implicit learning in a visuomotor adaptation task," *J. Neurophysiol.*, vol. 113, no. 10, pp. 3836–3849, Jun. 2015, doi: 10.1152/jn.00009.2015.
[9] Z. Bańkosz and S. Winiarski, "Kinematic Parameters of Topspin Forehand in Table Tennis and Their Inter-and Intra-Individual Variability," *J. Sports Sci. Med.*, vol. 19, no. 1, pp. 138–148, Mar. 2020.
[10] Y. He, G. Fekete, D. Sun, et al., "Lower Limb Biomechanics during the Topspin Forehand: A Systemic Review," *Bioengineering*, vol. 9, no. 8, p. 336, Jul. 2022, doi: 10.3390/bioengineering9080336.
[11] D. W. C. Wong, W. C. Lee, and W. K. Lam, "Biomechanics of Table Tennis: A Systematic Scoping Review of Playing Levels and Maneuvers," *Appl. Sci.*, vol. 10, no. 15, p. 5203, Jul. 2020, doi: 10.3390/app10155203.
[12] C. Y. Chou, Z. H. Chen, and Y. H. Sheu, "TTSwing: a Dataset for Table Tennis Swing and Racket Kinematics Analysis," *Sci. Data*, vol. 12, no. 1, p. 339, May 2025, doi: 10.1038/s41597-025-04680-y.
[13] S. Kidokoro, Y. Inaba, and K. Yoshida, "A topspin rate exceeding 110 rps reduces the ball time of arrival to the opponent," *Sports Biomech.*, vol. 24, no. 3, pp. 778–794, May 2025, doi: 10.1080/14763141.2022.2156916.
[14] M. Z. Chen, X. Wang, Q. Chen, et al., "An analysis of whole-body kinematics, muscle strength and activity during cross-step topspin among table tennis players," *Int. J. Perform. Anal. Sport*, vol. 22, no. 1, pp. 16–28, Feb. 2022, doi: 10.1080/24748668.2022.2025712.
[15] I. Malagoli Lanzoni, S. Bartolomei, and R. Di Michele, "Kinematic Analysis of the Racket Position during the Table Tennis Top Spin Forehand Stroke," *Appl. Sci.*, vol. 11, no. 11, p. 5178, Jun. 2021, doi: 10.3390/app11115178.
[16] Z. Li, L. Wang, L. Zhang, et al., "Effects of loop type and target direction variation on kinematics and kinetics of table tennis backhand loop," *Front. Bioeng. Biotechnol.*, vol. 13, p. 1722210, 2025, doi: 10.3389/fbioe.2025.1722210.
[17] Y. Iino, "Hip joint kinetics in the table tennis topspin forehand: relationship to racket velocity," *J. Sports Sci.*, vol. 36, no. 7, pp. 834–842, Apr. 2018, doi: 10.1080/02640414.2017.1344777.
[18] C. Mao, T. Liu, X. Li, et al., "A Comparative Biomechanical Analysis of Topspin Forehand against Topspin and Backspin," *Appl. Sci.*, vol. 13, no. 14, p. 8119, Jul. 2023, doi: 10.3390/app13148119.
[19] I. Malagoli Lanzoni, S. Bartolomei, R. Di Michele, et al., "Kinematic Analysis of the Racket Position during the Table Tennis Top Spin Forehand Stroke," *Appl. Sci.*, vol. 11, no. 11, p. 5178, Jun. 2021, doi: 10.3390/app11115178.
[20] D. W. Franklin and D. M. Wolpert, "Visuomotor feedback gains upregulate during the learning of novel dynamics," *J. Neurosci.*, vol. 32, no. 24, pp. 8542–8549, Jun. 2012, doi: 10.1523/JNEUROSCI.5785-11.2012.